Stalk Model of Membrane Fusion: Solution of Energy Crisis

Yonathan Kozlovsky and Michael M. Kozlov
Department of Physiology and Pharmacology, Sackler Faculty of Medicine, Tel-Aviv University, Ramat Aviv, Tel Aviv 69978, Israel

ABSTRACT Membrane fusion proceeds via formation of intermediate nonbilayer structures. The stalk model of fusion intermediate is commonly recognized to account for the major phenomenology of the fusion process. However, in its current form, the stalk model poses a challenge. On one hand, it is able to describe qualitatively the modulation of the fusion reaction by the lipid composition of the membranes. On the other, it predicts very large values of the stalk energy, so that the related energy barrier for fusion cannot be overcome by membranes within a biologically reasonable span of time. We suggest a new structure for the fusion stalk, which resolves the energy crisis of the model. Our approach is based on a combined deformation of the stalk membrane including bending of the membrane surface and tilt of the hydrocarbon chains of lipid molecules. We demonstrate that the energy of the fusion stalk is a few times smaller than those predicted previously and the stalks are feasible in real systems. We account quantitatively for the experimental results on dependence of the fusion reaction on the lipid composition of different membrane monolayers. We analyze the dependence of the stalk energy on the distance between the fusing membranes and provide the experimentally testable predictions for the structural features of the stalk intermediates.

INTRODUCTION

The ability to fuse is shared by biological membranes, consisting of phospholipid bilayers with embedded and bound membrane proteins, and by artificially formed purely lipid membranes. Normally, the membranes are mechanically stable. This is guaranteed by powerful hydrophobic effect (Tanford, 1980), which drives self-assembly of the lipid molecules into bilayer and maintains the bilayer integrity. Fusion involves drastic although local changes in the initial membrane structure. Obviously, the membrane configurations emerging at the intermediate stages of fusion require input of energy and, hence, represent energy barriers the membranes have to overcome on the way to the new fused state. These configurations referred to as the fusion intermediates largely limit the rate of the fusion reaction.

Modeling the lipidic fusion intermediates has a more than two decades history (Chernomordik et al., 1995a). Although, at the early stages, several different structures have been suggested, only one of them, called fusion stalk (Gingell and Ginsberg, 1978; Kozlov and Markin, 1983), is currently recognized to adequately describe the transition stage of membrane fusion (Chernomordik et al., 1995a; Jahn and Südhof, 1999).

Fusion stalk is a local lipidic connection between the proximal (contacting) monolayers of the fusing membranes (Fig. 1). At the stage of stalk formation, the distal monolayers of the membranes are still separated, and the achieved state is referred to as hemifusion. A physical model of the fusion process, based on this hypothetical intermediate and referred to as the stalk model, has been developed in a series of works (Kozlov and Markin, 1983; Markin et al., 1984; Chernomordik et al., 1985; Leikin et al., 1987; Kozlov et al., 1989), further modified by Siegel (1993, 1999) and, recently, by Kuzmin et al. (2001).

A number of important predictions of the stalk hypothesis have been verified experimentally for fusion of protein-free lipid bilayers and for some examples of biological fusion. To start with, the hypothesis suggests that merger of the proximal monolayers of the membranes precedes merger of their distal monolayers. Indeed, the existence of a distinct hemifusion stage has been documented for different experimental systems based on protein-free bilayers (Chanturiya et al., 1997; Chernomordik et al., 1995a, b; Lee and Lentz, 1997; Pantazatos and MacDonald, 1999) and for fusion of biological membranes (Chernomordik et al., 1998; Kemble et al., 1994; Leikina and Chernomordik, 2000; Melikyan et al., 1995; Song et al., 1991). Although these data substantiated the important positions of the model, more detailed theoretical analysis revealed major problem with the physical basis of the approach. Recent estimates (Siegel, 1993, 1999) suggested that the energy of the stalk intermediate is too high to allow its formation even for lipid membranes demonstrating very fast fusion, such as bilayers formed from dioleoylphosphatidylethanolamine (DOPE). Resolving this "energy crisis" has been of utmost importance for understanding physical mechanisms of stalk formation and membrane fusion.

In this work, we suggest a new structure for the stalk intermediate, which differs in important details from that considered previously. We demonstrate that the energy of this modified structure is considerably smaller than that previously obtained, so that the stalk intermediate can be formed in the experimental conditions. A remarkable result of our model is that the stalk energy practically does not depend on the distance between the fusing membranes. The

Submitted July 16, 2001 and accepted for publication November 16, 2001.
Address reprint requests to Michael M. Kozlov, Tel-Aviv University, Sackler Faculty of Medicine, Dept. of Physiol. & Pharmacol., Ramat-Aviv, Tel-Aviv 69978, Israel. Tel.: +972-3-640-7863; Fax: +972-3-640-9113; E-mail: misha@picard.tau.ac.il.

0006-3495/02/02/882/14 $2.00

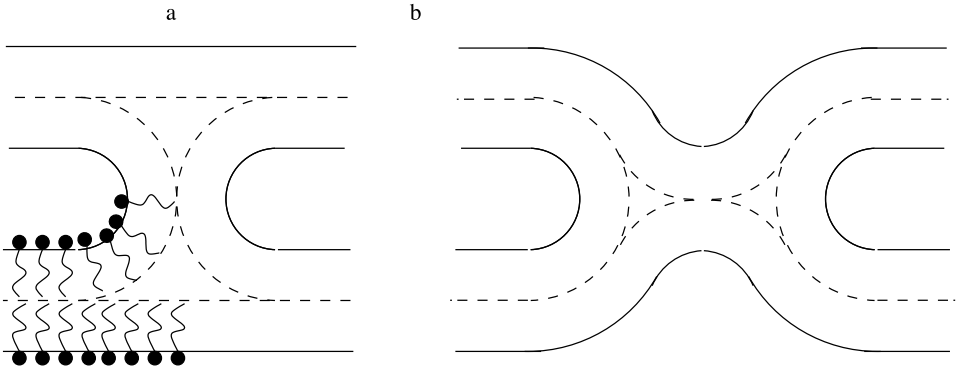

FIGURE 1 Previous model for stalk intermediates. (*a*) Fusion stalk. (*b*) Transmembrane contact (TMC). The structures are axially symmetric.

model accounts for the reported experimental data on modulation of the fusion reaction by lipid composition of the membrane monolayers and provides the experimentally testable predictions for the structural features of the stalk intermediate.

ENERGY CRISIS OF THE STALK MODEL

Criterion for energy of fusion intermediate

As mentioned above, the fusion intermediates are not supposed to represent the final structures adopted by the membranes. The energy of a fusion intermediate, F_{int}, may be larger than the energy of the initial membranes, F_0. In the case where F_{int} is too large compared to F_0, formation of the fusion intermediate becomes improbable. Estimations based on the experimental investigations of the electrical breakdown of membranes (Chernomordik and Abidor, 1980; Weaver and Mintzer, 1981) show (Kuzmin et al. 2001) that the maximal value of the relative energy, $F_{bar} = F_{int} - F_0$, that the membrane can overcome within a characteristic time scale of biological fusion is about $F_{bar} \approx 40kT$.

Energies predicted by the previous versions of the stalk model

Fusion of two initially separated membranes requires a number of steps, which include a local approach to small distances; some kind of perturbation of structure of the apposing monolayers such as, for example, their rupture in the region of the close contact; merger of the apposing monolayers; and formation of the lipid stalk between the membranes (Leikin et al. 1987). Because of complexity of quantitative evaluation of the early stages of fusion, the major efforts have been devoted to modeling the lipid stalk, whose energy is considered as a lower bound to the true energy barrier of the fusion reaction (Siegel, 1993; Chernomordik et al., 1995a).

Originally, the stalk membrane was assumed to have a semitoroidal shape (Fig. 1 *a*) (Kozlov and Markin, 1983). Depending on conditions, the stalk may have a tendency to expand, resulting in dimpling of the distal monolayers toward each other and formation of a hemifusion diaphragm (Kozlov and Markin, 1983; Markin et al. 1984). The intermediate structure of an early stage of stalk expansion was called the transmonolayer contact (TMC) (Siegel, 1993) (Fig. 1 *b*).

The most obvious feature of the stalk and TMC is a strongly curved shape of their membranes (Fig. 1). Therefore, the original version of the model (Kozlov and Markin, 1983; Markin et al. 1984; Leikin et al. 1987; Kozlov et al., 1989) was based on the analysis of the stalk bending energy. For a membrane composed of a lipid with common properties such as dioleoylphosphatidylcholine (DOPC), the energy of stalk was computed to be close to $40kT$, whereas formation of TMC required an additional increase of the energy. For a membrane consisting of DOPE, a lipid having an internal tendency to bend and form inverted hexagonal phase (Gruner et al. 1988; Rand et al., 1990), the stalk energy was estimated as only a few kT.

The further development of the stalk model by Siegel (1993, 1999) revealed an additional considerable contribution to the energy. It is related to the so-called hydrophobic interstices (Turner and Gruner, 1992), which result from packing the hydrocarbon chains of lipid molecules around the hydrophobic regions where the portions of differently curved lipid monolayers contact each other (Fig. 1). A tendency of the system to minimize the interstices results in bending of the distal membrane monolayers, another issue, which has been neglected in the original stalk model.

The value of the interstice energy can be estimated based on the experimental data on mesophase behavior of aqueous solutions of lipids (Siegel, 1993). The resulting overall energies of the fusion intermediates turned out to be much larger than originally predicted. For the aqueous distance of ~3 nm between the fusing membranes, which corresponds to an equilibrium intermembrane spacing in pure lipid systems (Rand and Parsegian, 1989), the stalk energies for membranes consisting of DOPC and DOPE were predicted

to equal 170kT and 150kT, respectively. Even few times larger stalk energies have been obtained for the aqueous distances between the membranes of ~10 nm (Siegel, 1993) corresponding to viral fusion (Skehel and Wiley, 2000).

Recently, another attempt has been undertaken to modify the stalk model (Kuzmin et al., 2001) based on a more sophisticated way to estimate the energies of the hydrophobic interstices. The authors have chosen to present the energy with respect to a hypothetical highly stressed dimpled state of the membranes. Relating their results to the initial flat shape of the membranes gives the stalk energy of more than 220kT, even exceeding the results of the modified model of Siegel (1999).

Challenge for the present research

Comparing the energies predicted by the modified model (Siegel, 1993, 1999) with the above criterion for fusion intermediate leads to the conclusion that the stalk cannot form in a real system. In contrast, membranes do fuse, and the major qualitative predictions of the original model (Kozlov and Markin, 1983; Markin et al., 1984; Chernomordik et al., 1985) on modulation of the fusion reaction by the membrane lipid composition have got a solid experimental confirmation (Chernomordik et al., 1995a). How to reconcile this inconsistency? A straightforward suggestion is that the structure of the stalk intermediates is different from that suggested previously. A more optimal structure possessing a smaller energy, which can be overcome due to thermal fluctuations or protein refolding has to be found. In the following, we propose and analyze such a structure.

STRUCTURE OF FUSION STALK

The excessive stalk energy predicted by the earlier analysis (Siegel, 1993) results from the energy price of the hydrophobic interstices, which have been extensively discussed in the context of packing the hydrocarbon chains of lipid molecules in the inverted hexagonal (H_{II}) phases (Gruner, 1989; Seddon, 1990; Turner and Gruner, 1992; Kirk et al., 1984; Tate and Gruner, 1987; Sjölund et al., 1989; Duesing et al., 1997; Rand and Fuller, 1994). Recently, a model of the H_{II} phase has been developed proposing that the hydrophobic interstices are filled due to tilting the hydrocarbon chains with respect to the monolayer surface (Hamm and Kozlov, 1998, 2000). This tilt model succeeded to interpret quantitatively the phase diagram of the aqueous solutions of glycolipids (Hamm and Kozlov, 1998).

We suggest the stalk structure based on the tilt model for the hydrophobic interstices, as illustrated in Fig. 2. To emphasize the major features of our model, let us compare Figs. 1 and 2. The hydrophobic void (Fig. 1) is filled (Fig. 2) due to an oblique packing of the hydrocarbon chains with respect to the membrane surface. This results in a sharp corner in the monolayer profile. In the cross-section of stalk,

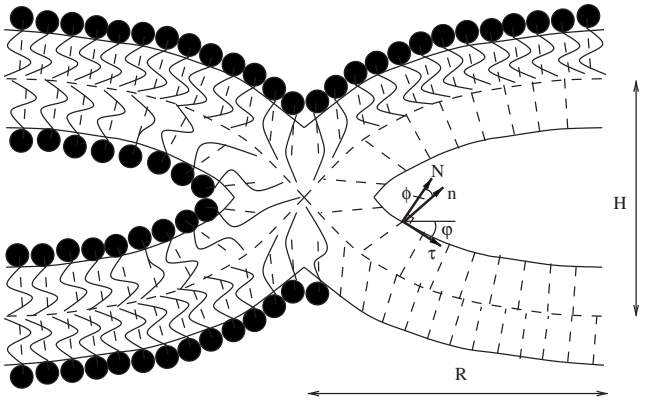

FIGURE 2 Tilt model for stalk and TMC. The shape is axially symmetric. Illustration of notations used: **N** is the unit vector of the normal to the monolayer surface, **n** is the director of a hydrocarbon chain, $\boldsymbol{\tau}$ is the tangential unit vector, φ is the tangential angle, ϕ is the tilt angle; H is the intermembrane distance; R is the stalk width. The presented relationship between the monolayer thickness and the dimensions of the hydrocarbon chains is approximately equal to the real one.

the corner is located between two adjacent molecules (Fig. 2) so that none of them suffers a strong bending. In addition to tilt of the hydrocarbon chains, the membrane is curved close to the corner (Fig. 2). The membrane curvature and tilt of the chains smoothly relax along the membrane surface to the flat state with vanishing tilt.

The illustration in Fig. 2 implies that several hydrocarbon chains terminate simultaneously at the center of the stalk structure. This may lead to chain-packing problems similar to those revealed by computer analysis of micellar structures, where only one chain has been shown to occupy the center of a micelle. However, the stalk structure (Fig. 2) is similar geometrically to the inverted hexagonal (H_{II}) phases rather than to micelles. Computer analysis of H_{II} phases (Gido et al., 1993) confirms a possibility of formation of sharp corners filled by hydrocarbon chains similar to that presented in Fig. 2.

Terminologically, the suggested structure (Fig. 2) is the fusion stalk and the TMC at the same time. Indeed, on one hand, it corresponds to the very first merger of the proximal monolayers of the fusing membranes and, on the other, the distal monolayers are already deformed in a way that they touch each other, although point-wise.

ELASTIC MODEL FOR STALK INTERMEDIATE

To proceed, we need a physical model describing the elastic energy of a complex deformation of the membrane monolayers, which involves bending of the monolayer surface and tilt of the hydrocarbon chains of lipid molecules.

Monolayer shape and deformations

We apply the approach developed in detail recently (Hamm and Kozlov, 1998, 2000), which is, in turn, based on the

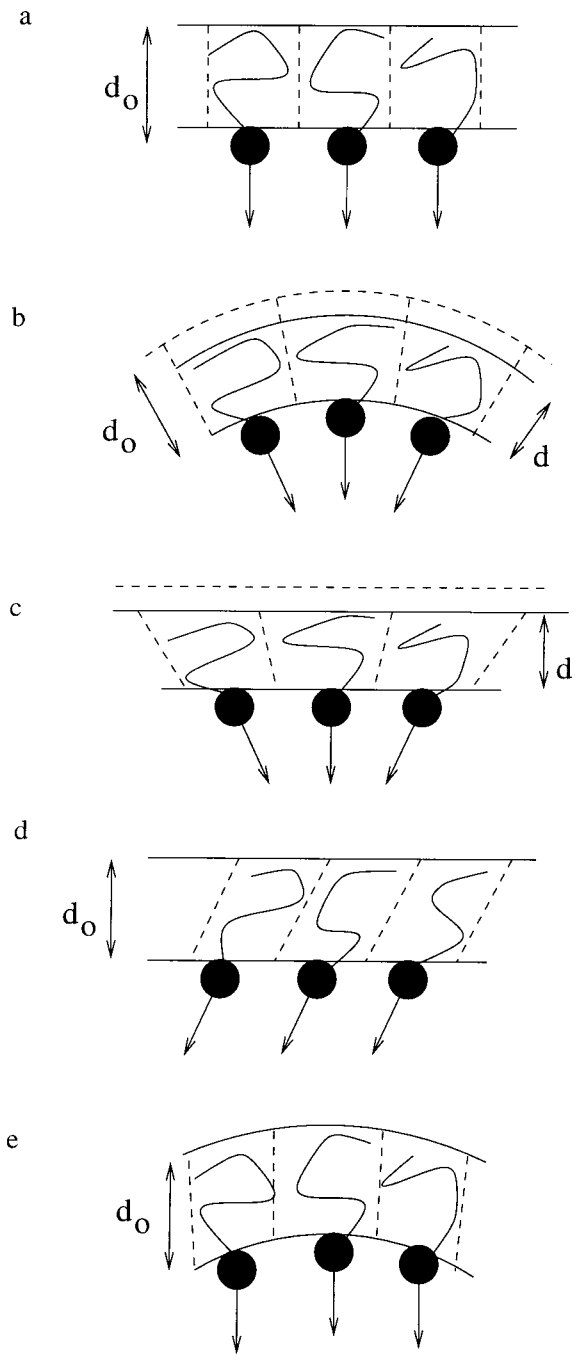

FIGURE 3 Deformations of a monolayer. (*a*) The initial undeformed state. (*b*) Bending with vanishing tilt. (*c*) Splay of the chains resulting from changing tilt in a flat monolayer. (*d*) Homogeneous tilt of the chains. (*e*) Mutual compensation of bending and tilt resulting in a bent membrane with vanishing splay of the chains.

ideas of the classical works by Frank (1958) and Helfrich (1973). We consider a lipid monolayer having, in the initial state, a flat shape (Fig. 3 *a*). To characterize the geometry of the monolayer, we use the dividing surface (Gibbs, 1876/78), which lies along the interface between the polar groups and the hydrophobic interior and has been shown for particular lipids to play a role of the neutral surface (Kozlov and Winterhalter, 1991a,b; Kozlov et al., 1994; Leikin et al., 1996). The monolayer shape will be identified with the shape of its dividing surface. To describe it mathematically, we define in each point of the dividing surface a unit normal vector **N** (Fig. 2).

The average orientation of a hydrocarbon chain is expressed by a unit vector **n** referred to as the chain director. In the initial state, the chains are perpendicular to the dividing surface, meaning that **n** coincides with **N** (Fig. 3 *a*). The area of the chain cross section at the dividing surface is denoted by a. We consider two deformations of the monolayer: bending, resulting in deviation of the monolayer shape from the initial flat one (Fig. 3 *b*); and tilt of the hydrocarbon chains, resulting in deviation of the chain director **n** from the surface normal **N** (Fig. 3, *c* and *d*). We will assume the chain area a to remain constant, meaning that the monolayer does not undergo lateral stretch, because the corresponding membrane rigidity (Rawicz et al., 2000) is considerably larger than those of tilt (Hamm and Kozlov, 1998, 2000) and bending (Niggemann et al., 1995).

The volume of a hydrocarbon chain, v, does not change in the course of membrane deformations, because the hydrocarbon moiety of a lipid molecule is practically incompressible. A simple geometrical consideration based on Fig. 3 *d*, and accounting for constancy of v and a, shows (Hamm and Kozlov, 2000) that the deformation of tilt results in stretch of the hydrocarbon chains with respect to their initial length. At the same time, the monolayer thickness measured perpendicularly to the membrane surface remains constant. The stretch of the chains accompanying their tilt allows for filling the hydrophobic voids of the stalk intermediate.

Elastic energy

The elastic energy of a monolayer originates primarily from the hydrocarbon chains (Helfrich, 1973; Ben-Shaul, 1995). Within the continuous description, the major contributions to the elastic energy arise, on one hand, from the splay of the chains (Frank, 1958; Helfrich, 1973) and, on the other, from uniform tilt of the chains with respect to the monolayer surface (MacKintosh and Lubensky, 1991).

Energy of splay

Splay of the hydrocarbon chains is illustrated in Fig. 3, *b* and *c*. It can result from two different deformations (Hamm and Kozlov, 1998, 2000): bending of the monolayer surface, whereas the hydrocarbon chains remain parallel to the surface normal, $\mathbf{n} = \mathbf{N}$, (Fig. 3 *b*), and variation of the molecular director **n** along the monolayer surface, whereas the surface remains flat (Fig. 3 *c*). This means that the chains exhibit tilt, $\mathbf{n} \neq \mathbf{N}$, which changes along the monolayer plane.

Obviously, combinations of these two deformations also result in splay of the chains. Mathematically, splay of the chains, denoted by $\tilde{J}$, can be presented for the two cases above and their combinations in the same form (Helfrich, 1973; Hamm and Kozlov, 2000)

$$\tilde{J} = \text{div } \mathbf{n}, \tag{1}$$

where div **n** denotes the covariant divergence of the director **n** along the monolayer surface. In the case, of pure bending, **n** = **N**, the splay (Eq. 1) is given by $\tilde{J}$ = div **N**, and, according to the general geometrical relationship, is equal to the total curvature, J, of the monolayer surface (Thomas, 1961). For the case of varying director, Eq. 1 is analogous to splay in a liquid crystal (Frank, 1958).

The energy of splay per unit area of the dividing surface can be expressed as (Hamm and Kozlov, 1998, 2000)

$$f_s = \tfrac{1}{2} \cdot \kappa \cdot (\text{div } \mathbf{n} - \tilde{J}_s)^2, \tag{2}$$

where $\tilde{J}_s$ is the spontaneous splay and κ is the splay modulus of the monolayer, the two characterizing the monolayer elastic properties. The spontaneous splay, $\tilde{J}_s$, coincides with the spontaneous curvature, J_s, introduced by Helfrich (1973) for the cases where splay originates solely from the monolayer bending. The spontaneous splay is related to the effective shapes of lipid molecules constituting the monolayer (Israelachvili et al. 1980; De Kruijff and Cullis, 1980). For a common lipid such as DOPC, the spontaneous splay is slightly negative, $\tilde{J}_s \approx -0.1$ nm^{-1} (Chen and Rand, 1997); for DOPE, this value is strongly negative, $\tilde{J}_s \approx -0.35$ nm^{-1} (Kozlov et al., 1994; Leikin et al., 1996); whereas, for lysolipids and, specifically, for lysophosphatidylcholine (LPC), the spontaneous splay is positive, $\tilde{J}_s \approx 0.26$ nm^{-1} (Fuller and Rand, 2001). The spontaneous splay of a mixed monolayer can be estimated as an average over the molecules constituting the monolayer (Kozlov and Helfrich, 1992).

The splay modulus κ coincides with the Helfrich bending modulus (Helfrich, 1973; Hamm and Kozlov, 2000). Its value, $\kappa = 10kT$, measured for monolayers (Niggemann et al., 1995; Leikin et al., 1996), will be used for calculations below.

The major assumptions of the model (Eq. 2) are that the hydrophobic moiety of a lipid monolayer can be described as an elastic continuum and that the splay is small compared to the monolayer thickness δ, so that $|\text{div } \mathbf{n}| \cdot \delta < 1$. While accounting for a combined deformation of bending and tilt, Eq. 2 represents the Helfrich elastic model (Helfrich, 1973) for the case of pure bending.

Energy of tilt

Uniform tilt of the hydrocarbon chains is illustrated in Fig. 3 *d*. Tilt can be quantified by a vector **t** defined as (MacKintosh and Lubensky, 1991; Hamm and Kozlov, 1998, 2000)

$$\mathbf{t} = \frac{\mathbf{n}}{\mathbf{n} \cdot \mathbf{N}} - \mathbf{N},$$

which is parallel to the dividing surface and characterizes the deviation of the director **n** from the surface normal **N** (Fig. 3 *d*). The corresponding energy per unit area of the monolayer is given by (MacKintosh and Lubensky, 1991; Hamm and Kozlov, 2000)

$$f_t = \tfrac{1}{2} \cdot \kappa_t \cdot \mathbf{t}^2, \tag{3}$$

where κ_t is the tilt modulus (Hamm and Kozlov, 2000). The major contribution to the tilt modulus κ_t results from the stretch of the hydrocarbon chains. This follows from comparison of the model estimation (Hamm and Kozlov, 2000) with the value of $\kappa_t = 0.04$ N/m, found from fitting the experimental results on phase transitions in lipid systems (Hamm and Kozlov, 1998). The latter value for the tilt modulus will be used for computations below. The quadratic model (Eq. 3) assumes small absolute values of tilt, $|\mathbf{t}| < 1$.

Main equations

We relate the total energy f_{tot} consisting of the energies of splay (Eq. 2) and uniform tilt (Eq. 3) to that of the initial flat state with vanishing splay and tilt, $\tilde{J} = 0$, $\mathbf{t} = 0$. The resulting energy per unit area of the monolayer is

$$f_{tot} = \tfrac{1}{2} \cdot \kappa \cdot (\text{div } \mathbf{n} - \tilde{J}_s)^2 + \tfrac{1}{2} \cdot \kappa_t \cdot \mathbf{t}^2 - \tfrac{1}{2} \cdot \kappa \cdot \tilde{J}_s^2. \tag{4}$$

To compute the total elastic energy of a monolayer, F_{mon}, the energy f_{tot} has to be integrated over the area A of the dividing surface,

$$F_{mon} = \int f_{tot} \, dA. \tag{5}$$

In Appendix A, we describe the details of calculation of the stalk energy.

ENERGY AND SHAPE OF STALK: RESULTS

Our analysis is aimed at describing the energy of the stalk intermediates formed in the course of different fusion reactions including, on one hand, fusion of pure lipid vesicles and, on the other, fusion of cell and viral membranes mediated by proteins. In each real system, there are constraints imposed on the configuration of the fusion site. We characterize these constraints by two parameters (Fig. 2). First, the distance R from the center of the stalk, to the region where membranes have to become flat and parallel, is referred as the width of the stalk base. Second, the distance

between the membrane middle planes H is referred to as the intermembrane distance. In the case of fusion of purely lipid membranes, the stalk width R is limited by the vesicular radius, which is usually larger than 100 nm. The intermembrane distance H, in this case, cannot become considerably smaller than its equilibrium value of ~6 nm (Rand and Parsegian, 1989), which is determined by the whole set of the interbilayer interactions.

In the case of fusion of biological membranes, the constraints for both H and R are determined by the protein architecture of the membrane contact and can vary considerably depending on the type of fusing cells or viruses. For example, in the case of fusion of influenza virus with target cell, the intramembrane distance H is determined by the length of HA molecule, $H \approx 13$ nm. The stalk intermediate is supposed to form within a membrane domain, which does not contain proteins (Kozlov and Chernomordik, 1998) so that the dimension of such domain limits the width of the stalk base R.

To be able to describe all possible types of fusion reaction, we analyze the stalk energy F for a large range of the intermembrane distances H and the stalk widths R. However, the calculations illustrating more special features of the model, such as dependence of the stalk energy on the spontaneous curvatures of the monolayers, will be performed for the equilibrium intermembrane distance $H = 6.2$ nm.

Symmetric membranes

To understand the major features of the fusion stalk, we first calculated its energy and structure for the case where the two membrane monolayers have the same spontaneous splay, $\tilde{J}_s = -0.1\ \mathrm{nm}^{-1}$, corresponding to the typical lipid DOPC. The values of the monolayer modulus of splay and tilt are taken to be $\kappa = 4 \times 10^{-20}\ J$ and $\kappa_t = 0.04$ N/m (Hamm and Kozlov, 2000).

Stalk energy

Dependence of the stalk energy F on the stalk width R and intermembrane distance H has the shape of a canyon, which descends monotonically with growing R and H. This means that the stalk has a general tendency to expand its base and length. If the geometrical constraints limiting R and H are lifted, what corresponds to fusion of giant vesicles, the stalk becomes infinitely wide ($R \to \infty$) and long ($H \to \infty$), and its energy approaches the value of ~$43kT$.

In the case where the expansion of the stalk base is limited by a specific width R, an optimal intermembrane distance H_{opt} exists providing the stalk with a minimal energy. Dependence of H_{opt} on the stalk width R is illustrated in Fig. 4 by diamonds, and the related variation of the stalk energy F along the bottom of the canyon is presented in Fig. 4 by stars. To demonstrate a strong increase of the elastic energy of the stalk, F, at small R and H_{opt}, we started

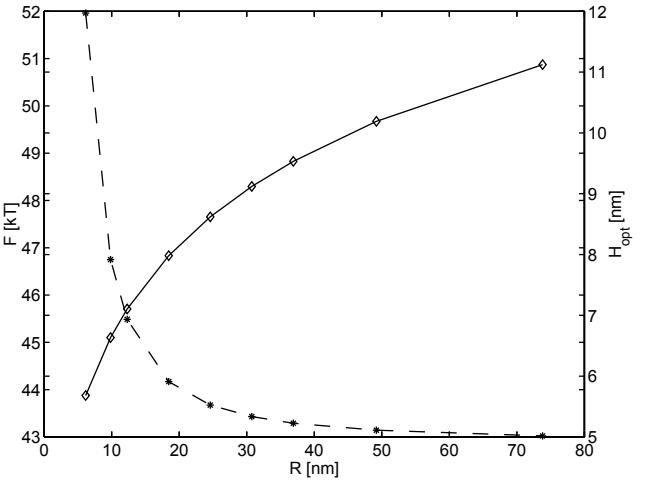

FIGURE 4 Dependence of the energy F (*) and the optimal intermembrane distance H_{opt} (◇) on the width of the stalk base, R.

our analysis from $H_{opt} = 5.7$ nm, which is slightly below the equilibrium intermembrane distance $H = 6.2$ nm (Rand and Parsegian, 1989). It should be noted that, within the small range of H between 5.7 nm and 6.2 nm, there is some positive contribution to the overall stalk energy from the repulsive interaction between the membranes. As a result, the whole energy of stalk in this region is slightly larger than that presented in Fig. 4 (*stars*) for 6 nm $< R <$ 8 nm.

If the stalk length is limited by a specific intermembrane distance H, the energy F decreases monotonically with growing width R, as represented in Fig. 5 for several values of H. The dependences $F(R)$ can be described by a characteristic stalk width R_c. We define R_c as a width where the slope of the curve $F(R)$ equals $(dF/dR)|_{R_c} = -1\ kT$/nm. The energy decreases sharply in a range of small stalk width, $R < R_c$, whereas, for the value of R exceeding the characteristic width, $R > R_c$, the energy changes slowly and reaches a plateau. The plateau value of the energy, F^*, depends on the intermembrane distance H, but this depen-

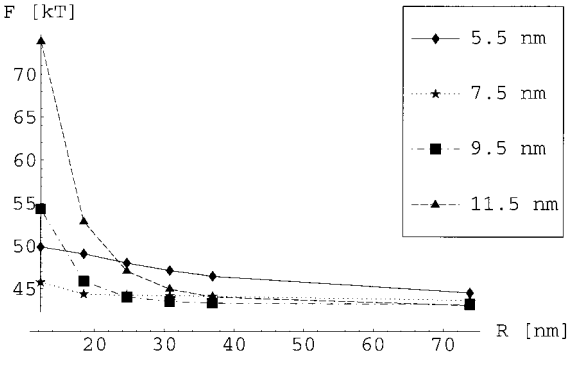

FIGURE 5 The dependence of the stalk energy F on the width of the stalk R for different values of the intermembrane distance H, as indicated in the figure.

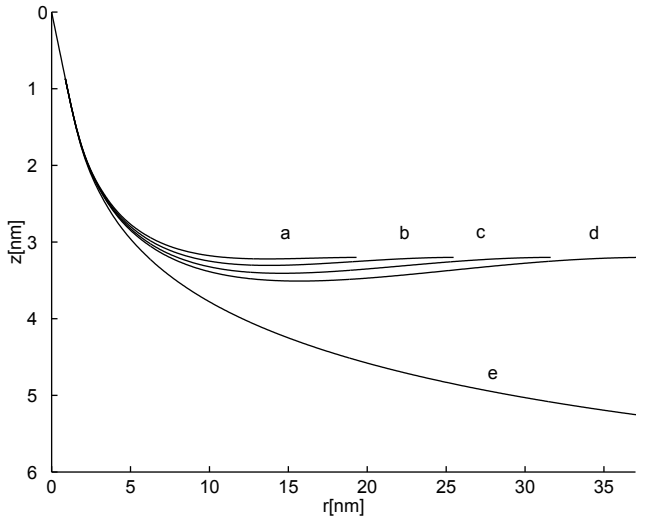

FIGURE 6 The shape of the stalk profile for constant intermembrane distance $H = 6.2$ nm and different values of the stalk width R. To emphasize the details of the shape, the scale along the z-axis is taken a few times smaller than that along the r-axis. (*a*) $R = 18$ nm; (*b*) $R = 25$ nm; (*c*) $R = 31$ nm; (*d*) $R = 37$ nm; (*e*) R and H are unconstrained.

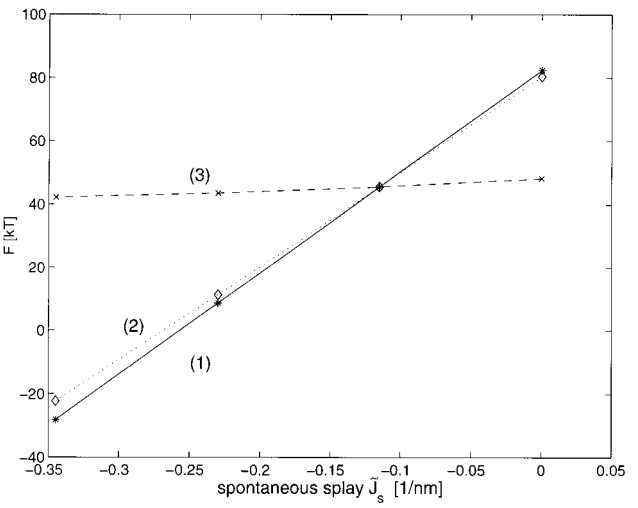

FIGURE 7 Dependence of the stalk energy F on the spontaneous splay $\tilde{J}_s$ of the membrane monolayers ($H = 6.2$ nm, $R = 25$ nm). (*1*) Symmetric membrane: the spontaneous splay is equal in the two monolayers. (*2*) Asymmetric membrane: F as a function of the spontaneous splay of the proximal monolayer, $\tilde{J}_s^p$, while the spontaneous splay of the distal monolayer is fixed, $\tilde{J}_s^d = -0.1\ \mathrm{nm}^{-1}$. (*3*) Asymmetric membrane: F as a function of the spontaneous splay of the distal monolayer, $\tilde{J}_s^d$, while the spontaneous splay of the proximal monolayer is fixed, $\tilde{J}_s^p = -0.1\ \mathrm{nm}^{-1}$.

dence is very weak and F^* remains below $47kT$ for all relevant values of H. The dependence of the characteristic width on the intermembrane distance, $R_c(H)$, can be described by

$$R_c = (2.4 \cdot H - 6.2)\ \mathrm{nm}. \quad (6)$$

The above definition for the characteristic width R_c is arbitrary. However, our numerical estimations show that, due to a well-pronounced distinction between the regions of a sharp and slow changes of the energy $F(R)$, the value of R_c is rather insensitive to the exact slope, $(\mathrm{d}F/\mathrm{d}R)|_{R_c}$, chosen for its determination.

Stalk configuration

The shape of the stalk surface depends on its width R and the intermembrane distance H. In Fig. 2, a characteristic shape of the stalk is presented. Change of the stalk shape with R and H is illustrated in Fig. 6 presenting the line whose revolution around the z-axis forms the midsurface of the half stalk. To emphasize the features of the stalk shape, the scale along the z-axis is chosen a few times smaller than that along the r-axis. For intermediate values of R and H, the stalk profile is nonmonotonic, exhibiting a depression before reaching the flat shape (Fig. 6, *a–d*). The depression becomes broader and deeper with increasing R. For an unconstrained stalk ($R \to \infty$, $H \to \infty$) the surface far from the stalk center approaches the shape of a catenoid (Fig. 6 *e*), the axially symmetric minimal surface characterized by zero total curvature (Nitsche, 1989). This unlimited catenoid-like shape has the energy of $\sim 43kT$ mentioned above.

Effects of spontaneous splay

We have computed the influence of the spontaneous splay of the membrane monolayers on the stalk energy for different values of the stalk width R and intermembrane distance H. Within an experimentally relevant range, the qualitative character of this influence turned out to be independent of the specific values of R and H. We present the results (Fig. 7) for the intermembrane distance $H = 6.2$ nm, corresponding to the equilibrium separation in the lamellar phases of egg phosphatidylcholine (Rand and Parsegian, 1989), and the stalk width $R = 25$ nm, which exceeds the characteristic width, R_c.

The dependence of the stalk energy F on the spontaneous splay of the monolayers, $\tilde{J}_s$, is represented by Fig. 7 (*line 1*) and is well described by $F = (82 + 261 \cdot \tilde{J}_s \cdot \delta) \cdot kT$, where δ is the distance between the monolayer neutral surface and the bilayer midplane, $\delta \approx 1.2$ nm. For the membrane of DOPC, having $\tilde{J}_s \approx -0.1\ \mathrm{nm}^{-1}$ (Chen and Rand, 1997), the stalk energy is about $F \approx 45kT$, which exceeds, by $\sim 5kT$, the above criterion of stalk formation due to thermal fluctuations. For DOPE characterized by a spontaneous splay of $\tilde{J}_s \approx -0.35\ \mathrm{nm}^{-1}$ (Kozlov et al., 1994; Leikin et al., 1996) the stalk energy is strongly negative, $F \approx -30kT$, meaning that, for this lipid, the stalk is energetically favorable and, hence, does not contribute to the energy barrier of membrane fusion. The spontaneous splay of a mixture of differ-

ent phospholipids can be calculated in a good approximation as a weighted average of the spontaneous splays of the components (see, for example, Kozlov and Helfrich, 1992). For example, the energy of a stalk consisting of a DOPE/DOPC mixture has a value intermediate between the energies of the pure DOPE and DOPC stalks, as represented in Fig. 7 by points on the line (*1*) corresponding to the weighted spontaneous splays.

Asymmetric membranes

The spontaneous splays of the two membrane monolayers have different effect on the overall stalk energy F. To analyze this issue, we performed computations for asymmetric stalk membrane. Line (*2*) in Fig. 7 represents the dependence of F on the spontaneous splay of the proximal monolayer, $\tilde{J}_s^p$, while that of the distal monolayer remains constant, $\tilde{J}_s^d = -0.1\ \mathrm{nm}^{-1}$. The function $F(\tilde{J}_s^p)$ practically coincides with the energy of a symmetric membrane Fig. 7, (*line 1*). In contrast, the dependence of the energy F on the spontaneous splay of the distal monolayer, $\tilde{J}_s^d$, turns out to be very weak. This is illustrated by line (*3*) in Fig. 7, which presents $F(\tilde{J}_s^d)$ at a fixed spontaneous splay of the proximal monolayer, $\tilde{J}_s^p = -0.1\ \mathrm{nm}^{-1}$. The results, Fig. 7 (*lines 2* and *3*), show that the major factor influencing the stalk energy is the spontaneous splay of the proximal monolayer, $\tilde{J}_s^p$, whereas the distal monolayer practically does not contribute to the effect of the spontaneous splay.

DISCUSSION

We suggest a new structure for the stalk intermediate of membrane fusion (Fig. 2), which resolves the energy crisis identified in the earlier models. Our model adequately interprets the experimental results on dependence of fusion on the lipid composition of different membrane monolayers, and gives experimentally testable predictions on the configuration of the fusion stalk.

Comparison with previous models

Why does the suggested approach succeed in solving the energy crisis? The major feature of the present model is that the deformations of the two membrane monolayers are not limited by bending, as previously assumed (Kozlov and Markin, 1983; Markin et al., 1984; Siegel 1993, 1999), but involve also tilt of the hydrocarbon chains (Hamm and Kozlov, 1998, 2000). The tilt plays a role of an additional internal degree of freedom of the monolayers and allows them to relax the overall energy. Specifically, tilt of the chains results in three effects influencing the monolayer energy. 1) The hydrophobic voids are filled by the hydrocarbon material so that no "vacuum" is created in the system. The stretch of the hydrocarbon chains necessary to fill the voids is implicated in the chain tilting, and the related energy is accounted by the tilt elasticity κ_t. 2) the overall area of the stalk monolayers is reduced compared to the initially proposed semitoroidal shape (Fig. 1) due to creation of a corner in the middle of the structure (Fig. 2). 3) Splay of the hydrocarbon chains resulting from tilt compensates, at least partially, for the splay produced by the monolayer bending (Fig. 3 *e*). In the modified stalk model of Siegel (1993, 1999), the tilt degree of freedom has not been considered at all and, therefore, the predicted energy was more than four times larger than that obtained in the present work.

In the recent model by Kuzmin et al. (2001), the distal monolayers of the stalk are assumed to undergo a localized tilt-like deformation, while the hydrocarbon chains of the proximal monolayer were not allowed to tilt. Because of these assumptions, the effect of tilt is drastically limited: the hydrophobic interstices are only partially filled, still leaving vacuum voids; the area of the strongly bent proximal monolayers, which have a semitoroidal shape, is the same as in the previous models, and, finally, the bending stresses are not compensated by the tilt-induced splay. If the stalk energy resulting from the model by Kuzmin et al. (2001) is related to the initial flat shape of the membrane, it turns out to exceed the results of Siegel (1999) and to be at least five times larger than the energy predicted by the present approach. As a result, the stalk structure suggested in Kuzmin et al. (2001) is far from being the lowest energy fusion intermediate.

Effects of different lipids

According to the experimental data accumulated over the last decades, different phospholipids exhibit distinct properties with respect to membrane fusion. The lipid DOPC forms, in aqueous solutions, stable lamellar phases, where the flat lipid bilayers separated by thin (2- to 3-nm) water gaps do not demonstrate any tendency to fuse spontaneously (Rand and Parsegian, 1989). However, addition to these systems of hydrocarbon solvent induces transformation of the lamellae into cylindrical membranes of the inverted hexagonal (H_{II}) phase (Sjölund et al., 1989), the process including multiple fusion of the initial membranes (Siegel et al., 1989; Siegel and Epand, 1997; Siegel, 1999). The aqueous solutions of DOPE form the H_{II} phase in normal conditions at room temperature without any additions. This lipid exhibits a temperature-driven spontaneous transition from lamellar to inverted hexagonal structure at $\sim$10°C (Gawrisch et al., 1992). This implies that, beginning from this temperature, the DOPE monolayers have a tendency to fuse spontaneously. Indeed, DOPE and other lipids supporting H_{II} phase formation (e.g., unsaturated fatty acids and diacylglycerol) promote fusion of protein-free bilayers and protein-mediated fusion (Basanez et al., 1998; Chernomordik et al., 1995a; Chernomordik et al., 1997; Walter et

al., 1994). In contrast, lysolipids, such as LPC, inhibit fusion. Addition of LPC to model (Chernomordik et al. 1985; Basanez et al., 1998; Chernomordik et al., 1994) and biological (Chernomordik et al., 1995a; Chernomordik et al., 1997; Gaudin, 2000; Melikyan et al., 2000) membranes considerably inhibited the fusion reaction.

Promotion and inhibition of fusion by different lipids correlate with their molecular structure, which can be characterized by the effective molecular shape (Israelachvili et al., 1980; De Kruijff and Cullis, 1980; Chernomordik et al., 1985) or, alternatively, the spontaneous curvature, J_s (Helfrich, 1973). The notion of the spontaneous curvature, J_s, has been recently generalized to the spontaneous splay, $\tilde{J}_s$ (Hamm and Kozlov, 1998, 2000). The spontaneous splay of DOPE measured experimentally (Rand and Fuller, 1994; Kozlov et al., 1994; Leikin et al., 1996) is strongly negative, $\tilde{J}_s^{DOPE} = -1/2.8\ nm^{-1}$; for DOPC, this value can be estimated (Chen and Rand, 1997) as slightly negative, $\tilde{J}_s^{DOPC} = -1/8.7\ nm^{-1}$; and for LPC, the spontaneous splay is positive, $\tilde{J}_s^{LPC} = 1/3.8\ nm^{-1}$ (Fuller and Rand, 2001). Summarizing the experimental results, the more negative the spontaneous splay of a lipid is, the stronger is its propensity to fuse so that the lipids with the spontaneous splay close to $\tilde{J}_s \approx -0.3\ nm^{-1}$ exhibit spontaneous fusion.

The stalk model proposed in the present study readily interprets the dependence of membrane fusion on the lipid composition. For the DOPC membranes, our model predicts the energy of the stalk/TMC close to $F^{DOPC} \approx 45kT$. This energy is $\sim 5kT$ larger than F_{bar}, meaning that fusion should be an extremely rare event. This agrees with a general stability of the DOPC lamellar phases (Rand and Parsegian, 1989). In contrast, this energy can be easily decreased to a value below F_{bar} to allow for fusion. This can be done by a suitable change in the system compositions such as addition of a hydrocarbon solvent (Sjölund et al., 1989), which is supposed to enter the hydrophobic interstices and partially relieve the membrane stresses. The energy of a stalk intermediate we predict for the DOPE membranes is negative $F^{DOPE} \approx -30kT$, which explains the strong tendency of these membranes to fuse. And, finally, a growth of the stalk energy with increasing spontaneous splay (Fig. 7 (*line 1*)) explains the effective inhibition of fusion by additions of LPC to the membrane monolayers (Chernomordik et al., 1995a).

Effects of different monolayers

Another result of our model is a prediction of a different influence on stalk formation of the spontaneous splay, $\tilde{J}_s$, of the proximal and distal membrane monolayers. According to the earlier model (Siegel, 1993), changes in $\tilde{J}_s$ of the two monolayers exert a similar effect on the stalk energy F. In contrast, our calculations show that the dependence of the energy F on $\tilde{J}_s$ is related almost solely to the proximal monolayer (Fig. 7 (*lines 2* and *3*)). Changes in the spontaneous splay of the distal monolayer, practically, do not influence the energy (Fig. 7 (*line 3*)). In agreement with our prediction, the experimental investigations showed that additions of LPC to the proximal monolayer considerably inhibited hemifusion, whereas insertion of the same molecules to the distal monolayer had practically no effect on membrane hemifusion (Chernomordik et al., 1997; Chernomordik et al., 1998).

Effects of stalk dimensions

Our model predicts that, for every given inter-membrane spacing H, the stalk tends to expand its base, thus, increasing the width R (Fig. 5). But the force driving this expansion is strong only as long as the width is smaller than the characteristic value, $R < R_c$. For larger values of the width, $R > R_c$, the stalk energy almost does not change and, hence, the driving force for the expansion of the stalk base is very small. In practical terms, this means that the stalk tends to expand up to the characteristic width R_c, which has values close to the intermembrane distance H (Eq. 6). This result of the model can be verified experimentally.

How does the stalk energy depend on the intermembrane distance H? This question is important for comparing fusion in different systems. Indeed, in the pure lipid systems, the typical intermembrane spacing is $\sim$6 nm (Rand and Parsegian, 1989), whereas the distance between fusing cell membranes determined by membrane proteins constitutes up to 12 nm (Skehel and Wiley, 2000). Earlier versions of the stalk model predicted a drastic increase in the energy with the intermembrane distance H (Siegel, 1993, 1999). This would imply that the architecture of the fusion intermediate in the pure lipidic membrane system should differ from that formed between cell membranes. In contrast, our model predicts practically the same energy for the fusion intermediates of different intermembrane distances, provided that all of them can expand laterally reaching the width of R_c. The energy of a stalk with $H = 12$ nm turns out to be even $1.5kT$ smaller than that of stalk with $H \approx 6$ nm. Hence, all the results of our model are valid for different intermembrane distances.

If the width of the stalk base is restricted to values smaller than the characteristic one, $R < R_c$, the stalk energy increases with the intermembrane distance H (Fig. 5). This can be expected for fusion of influenza virus, whose membrane contains a high density of the fusion protein HA. The lateral spacing between the HA molecules available for stalk formation is close to $R \approx 7$ nm (Taylor et al., 1987), whereas the intramembrane distance, as determined by the length of the HA ectodomains, is $H \approx 13$ nm (Bullough et al., 1994). According to Eq. 6, in this case, the stalk base does not reach the characteristic width. To avoid a large energy barrier in such a situation, the stalk formation has to be preceded by decrease in H due to dimpling of the

membranes toward each other, as suggested in Kozlov and Chernomordik (1998).

Assumptions of the model

The suggested model includes several assumptions, which have to be discussed. We use a continuum description of a lipid monolayer, analogous to the Frank theory of liquid crystals (Frank, 1958) and the Helfrich theory of membrane elasticity (Helfrich, 1973). Such description requires, in general, the length scale of deformations to be considerably larger than the dimension of particles constituting the system. The role of such particles in our case is played by the hydrocarbon chains, and the particle dimension is the diameter of the chain projection on the membrane plane, which equals ~0.6 nm. According to our results (Fig. 2), the deformation of splay of the stalk monolayers extends over 7–8 hydrocarbon chains, meaning that its length scale is only several times larger than the particle dimension. The deformation of tilt of the stalk intermediate turns out to be even more concentrated and extends over 2–3 hydrocarbon chains. Although the macroscopic theories are often applied in similar cases, the validity of the results is always questionable and has to be verified by comparison with experimental data. A continuum elastic approach of the present work has been used previously for analysis of the energy and the elastic behavior of the inverted hexagonal (H_{II}) phases (Kozlov and Winterhalter, 1991a,b; Kozlov et al., 1994; Leikin et al., 1996; Hamm and Kozlov, 1998), where the ratio between the scale of the monolayer deformations and the chain dimension is the same as for the stalk intermediate. This approach proved to describe quantitatively the experimental data on the lamellar–hexagonal phase transitions and the stress–strain relationships of the H_{II} phases. This convinces us that, in spite of the general reservations above, our continuum model adequately describes the stalk intermediate.

We make an unusual assumption that the profile of the stalk membrane exhibits a sharp corner. To a first glance, this corresponds to an infinite membrane curvature ($J \to \infty$), which is concentrated within a vanishing area ($a \to 0$). However, consideration of the structure of the corner in terms of deformations of tilt and splay of the hydrocarbon chains shows that the chains do not exhibit infinite splay at the corner (Fig. 2). At the same time, the finite splay, analogous to finite curvature, and finite tilt of the hydrocarbon chains in the region of the corner are taken into account by integrating the energy (Eq. 4) up to the corner. Yet, an additional energy related to the sharp corner may originate from a repulsive interaction between the polar groups of the lipid molecules, resulting, for example, from hydration repulsion (Rand and Parsegian, 1989; Leikin et al., 1993) or the electrostatic interaction. Because this energy is a part of the energy of membrane deformations, to calculate its value, one needs a theory accounting for contribution of the hydration and electrostatic forces to the elastic characteristics of membranes.

We are not aware of any systematic treatment of the influence of hydration forces on the elastic moduli of membranes. However, a general idea about these effects can be based on the existing models for the hydrations forces (Appendix C). Based on the qualitative consideration of Appendix C, we assume that the hydration of the polar heads provides a negligible contribution to the stalk elastic energy.

A model for contributions of the electrostatic interaction to the membrane elasticity has been developed only for small curvatures of the membrane surface (Winterhalter and Helfrich, 1988), and, hence, it cannot describe the energy of the corner. We do not consider these effects, assuming the corner to be situated between adjacent uncharged polar heads.

The elastic model (Eq. 4) assumes the deformations of splay and tilt to be smaller than one, $|\mathrm{div}\ \mathbf{n} \cdot \delta| < 1$, $|\mathbf{t}| < 1$, where δ is the monolayer thickness. In reality, in our calculations, the deformations of tilt and dimensionless splay approach but never exceed the value of one in a very narrow region close to the corner of the stalk structure. To assure fulfillment of this condition, we limited the ranges of variations of parameters in our numerical procedure.

Another assumption of our calculation is that, on one hand, the neutral surfaces of the two membrane monolayers are parallel to the membrane midplane, and, on the other, the molecular areas on the neutral surfaces are constant along the whole membrane. Because of the relationship among the molecular volume, molecular area, and the splay of the hydrocarbon chains (Hamm and Kozlov, 2000), this assumption means that the molecular volume is not strictly conserved in the regions with splay. However this effect turns out to be of a higher order with respect to the dimensionless splay. Contributions of this order are not taken into account by our Hamiltonian (Eqs. 2 and 4). Nevertheless, to estimate the error related to these assumptions, we have numerically computed the deviations of the monolayer surfaces from the supposed shape, as required by conservation of the molecular volume. We have calculated the related change of the monolayer curvatures and the resulting energy. The determined maximal error of our results constitutes 5%.

We did not account in our model for the energy of the saddle-splay deformation (Frank, 1958; Helfrich, 1973) of the stalk monolayer, which is determined by a combination of the deformations of monolayer bending and tilt of the hydrocarbon chains (Hamm and Kozlov, 2000). The saddle splay is analogous in the case of simple bending to the Gaussian curvature of the monolayer surface. The value of the elastic modulus, $\bar{\kappa}$, determining the energy of the saddle-splay deformation of a monolayer is largely unknown (Ben-Shaul, 1995). We are not aware of any experimental investigations that have directly attempted to obtain $\bar{\kappa}$ of a

monolayer. The numerical calculations have been performed for contribution of the hydrocarbon chains to $\bar{\kappa}$ and have shown that its value constitutes less than 10% of the bending modulus κ (Szleifer et al., 1990). Based on these results, our estimation of a possible contribution of the saddle-splay deformation to the stalk energy did not exceed few percents of the energy of splay.

CONCLUSIONS

To conclude, the present work resolves the energy crisis of the stalk model of membrane fusion. We suggest a specific structure of the stalk intermediate where the major roles are played by deformations of tilt and splay of the hydrocarbon chains. We demonstrate that the stalk intermediates have energies much smaller than those predicted previously and can be formed in real systems due to thermal fluctuations of the membranes. The obtained dependence of the stalk energy on the lipid compositions of the membrane monolayers agrees with the existing experimental data. We predict that the stalk energy, practically, does not depend on the intramembrane distance, provided that the stalk base is sufficiently free to expand in the lateral direction.

APPENDIX A

Detailed form of equations and boundary conditions

Lipid monolayers forming the stalk have axially symmetric shapes (Fig. 2). To present mathematically the dividing surface of such a monolayer, we use the radial coordinate r and the tangential angle φ between the radial direction $\mathbf{r}$ and the unit vector $\boldsymbol{\tau}$ tangential to the surface as illustrated in Fig. 2. The dependence $\varphi(r)$ determines the shape of the dividing surface.

To express the tilt of the hydrocarbon chains, $\mathbf{t}$, we determine the tilt angle $\phi(r)$ between the chain director $\mathbf{n}$ and the normal to the surface $\mathbf{N}$ (Fig. 2). The absolute value of the tilt vector is

$$|\mathbf{t}| = \tan\phi_t. \tag{A1}$$

Splay (Eq. 1) of the hydrocarbon chains can be expressed as (Appendix B)

$$\operatorname{div}\mathbf{n} = \cos\varphi\cdot\frac{1}{r}\frac{\mathrm{d}(r\sin\phi)}{\mathrm{d}r} + \cos\phi\cdot\frac{1}{r}\frac{\mathrm{d}(r\sin\varphi)}{\mathrm{d}r}. \tag{A2}$$

According to Eq. A2, for the case of pure bending (Fig. 3 *b*) with vanishing tilt angle, $\phi = 0$, the splay adopts a familiar form of the total curvature of an axially symmetric surface,

$$\operatorname{div}\mathbf{n} = \frac{1}{r}\frac{\mathrm{d}(r\sin\varphi)}{\mathrm{d}r},$$

(see for example Helfrich, 1990). In the case of a flat surface, $\varphi = 0$ (Fig. 3 *c*), splay is generated by the change of the tilt angle,

$$\operatorname{div}\mathbf{n} = \frac{1}{r}\frac{\mathrm{d}(r\sin\phi)}{\mathrm{d}r}.$$

And, finally, the tangential angle and the tilt angle can cancel each other, $\varphi = -\phi$. As a result, the bent surface is characterized by a vanishing splay of hydrophobic chains, $\operatorname{div}\mathbf{n} = 0$. This configuration is illustrated in Fig. 3 *e*.

The elastic energy per unit area of the dividing surface of a monolayer, accounting for Eqs. 4, A1, and A2, is

$$f_{tot} = \frac{1}{2}\cdot\kappa\cdot\left[\cos\varphi\cdot\frac{1}{r}\frac{\mathrm{d}(r\sin\phi)}{\mathrm{d}r} + \cos\phi\cdot\frac{1}{r}\frac{\mathrm{d}(r\sin\varphi)}{\mathrm{d}r} - J_s\right]^2 + \frac{1}{2}\cdot\kappa_t\cdot(\tan\phi)^2 - \frac{1}{2}\cdot\kappa J_s^2. \tag{A3}$$

Aim of analysis

The shape of a lipid bilayer is represented by its middle plane and described by the dependence of the tangential angle of the middle plane φ_B (Fig. 2) on the radial coordinate, $\varphi_B(r)$. The dividing surfaces of the two lipid monolayers are assumed to be parallel to the middle plane. Hence, the tangential angles of the proximal, $\varphi_p(r)$, and distal, $\varphi_d(r)$, monolayers are directly related to $\varphi_B(r)$ of the middle plane (Appendix B). The tilt angles in the proximal, $\phi_p(r)$, and distal, $\phi_d(r)$, monolayers are independent functions. The energy of a bilayer is the sum of the energies (Eq. 5) of the two monolayers. The aim of our analysis is to compute the stalk energy, F, and to determine the shape of the stalk membrane, $\varphi_B(r)$, and distribution of tilt in its monolayers, $\phi_p(r)$ and $\phi_d(r)$.

Outline of analysis

The energy F, as obtained by integrating Eq. A3 over the areas of the membrane monolayers, depends on the functions $\varphi_B(r)$, $\phi_p(r)$, and $\phi_d(r)$. To find the membrane shape, $\varphi_B(r)$, and the distribution of tilt of the hydrocarbon chains, $\phi_p(r)$ and $\phi_d(r)$, we have to minimize the energy $F[\varphi_B(r), \phi_p(r), \phi_d(r)]$ with respect to these functions.

In the course of minimization, several conditions have to be satisfied:

- To ensure that the hydrophobic interstices are filled by the hydrocarbon chains, we set the tilt angles in the center of the stalk, $\mathbf{r} = 0$, as $\phi_d(r = 0) = -\pi/4$, and, $\phi_p(r = 0) = \pi/4$ (Fig. 2). This also accounts for finite values of splay in the corner.
- We require that, at the distance $r = R$ from the center of the stalk, the membranes become flat and parallel with the distance between the membranes' middle planes equal to H.
- Far from the stalk center, we require that the tilt of the hydrocarbon chains vanishes, $\mathbf{t}(r \to \infty) = 0$.

We calculate the energy and the structure of the stalk intermediate as a function of the following parameters dependent on the membrane properties, which can be modified in the experiments: the spontaneous curvatures J_s of the membrane monolayers, and the geometrical constraints imposed on the membranes, namely, the distance H between the membranes and the stalk width R. We perform the calculation numerically by the method of finite elements, which is equivalent to solving the Euler–Lagrange equations. The natural length scale of our calculation is determined by the thickness of the hydrophobic part of lipid monolayer, δ. We take egg phosphatidylcholine as a typical lipid and use for calculations the values of its geometrical parameters, and, specifically, $\delta = 1.2$ nm (Rand and Parsegian, 1989).

APPENDIX B

Geometrical relationships

Expression for splay

In this section, we express the splay of the hydrocarbon chains, $\operatorname{div}\mathbf{n}$, through the tangential angle of the membrane profile, φ, and the tilt angle,

ϕ (Fig. 2). We consider two lateral unit vectors in the meridional, $\mathbf{e}_\varphi$, and equatorial, $\mathbf{e}_\theta$, directions. The vector $\mathbf{e}_\varphi$ coincides with the tangential vector $\boldsymbol{\tau}$ defined in Appendix A (Fig. 2).

The lateral covariant divergence of the chain director representing the splay can be calculated according to

$$\mathrm{div}\ \mathbf{n} = \frac{\mathrm{d}\mathbf{n}}{\mathrm{d}s_\varphi}\mathbf{e}_\varphi + \frac{\mathrm{d}\mathbf{n}}{\mathrm{d}s_\theta}\mathbf{e}_\theta, \tag{B1}$$

where s_φ and s_θ are the arc lengths measured along the meridional and equatorial directions, respectively. The chain director can be presented as

$$\mathbf{n} = \cos\phi\cdot\mathbf{N} + \sin\phi\cdot\mathbf{e}_\varphi, \tag{B2}$$

so that its differential is

$$\mathrm{d}\mathbf{n} = \cos\phi\cdot\mathrm{d}\mathbf{N} + \sin\phi\cdot\mathrm{d}\mathbf{e}_\varphi - \sin\phi\cdot\mathbf{N}\cdot\mathrm{d}\phi + \cos\phi\cdot\mathbf{e}_\varphi\cdot\mathrm{d}\phi. \tag{B3}$$

The differential of the normal and the tangential meridional unit vectors are

$$\mathrm{d}\mathbf{N} = \mathbf{e}_\varphi\cdot\mathrm{d}\varphi + \sin\varphi\cdot\mathbf{e}_\theta\cdot\mathrm{d}\theta, \tag{B4}$$

$$\mathrm{d}\mathbf{e}_\varphi = -\mathbf{N}\cdot\mathrm{d}\varphi + \cos\varphi\cdot\mathbf{e}_\theta\cdot\mathrm{d}\theta. \tag{B5}$$

The differentials of the arc length in the meridional and equatorial directions are give by

$$\mathrm{d}s_\varphi = \frac{\mathrm{d}r}{\cos\varphi} \tag{B6}$$

and

$$\mathrm{d}s_\theta = r\cdot\mathrm{d}\theta. \tag{B7}$$

Inserting Eqs. B3–B7 into Eq. B1, we obtain for the splay

$$\mathrm{div}\ \mathbf{n} = \cos\phi\cdot\cos\varphi\cdot\frac{\mathrm{d}(\varphi+\phi)}{\mathrm{d}r} + \frac{\sin(\varphi+\phi)}{r}. \tag{B8}$$

The expression (B8) can be presented in a slightly different form (Eq. A2).

Relationship between the tangential angles of the monolayers and the bilayer midplane

The tangential angles of the proximal, $\varphi_\mathrm{p}(r)$, and distal, $\varphi_\mathrm{d}(r)$, monolayers are related to that of the bilayer middle plane $\varphi_\mathrm{B}(r)$ by

$$\varphi_\mathrm{p}(r + \delta\cdot\sin\varphi(r)) = \varphi_\mathrm{B}(r),$$
$$\varphi_\mathrm{d}(r - \delta\cdot\sin\varphi(r)) = -\varphi_\mathrm{B}(r). \tag{B9}$$

APPENDIX C

Qualitative consideration of effects of hydration forces

According to the established view (Marčelja and Radić, 1976; Gruen and Marčelja, 1983; Leikin et al. 1993), the hydration layer of a membrane is a layer of polarized water, which tends to decay exponentially in the direction perpendicular to the membrane surface. This layer has been described by a liquid crystal-like model (Marčelja and Radić, 1976) with water polarization playing a role of the order parameter. This approach successfully treated the hydration repulsion between apposing membranes (Gruen and Marčelja, 1983). Extending, in the spirit of Frank (1958), this liquid–crystalline model to description of deformations of splay and tilt of the hydration layer, one obtains a Hamiltonian analogous to Eq. 4, where the elastic coefficients account for the interactions between the polarized water molecules.

This model predicts that, in the vicinity of the corner, the water polarization can avoid infinite splay by tilting with respect to the membrane surface, analogously to the deformation of the hydrocarbon tails we considered above. This allows avoiding a seemingly infinite energy of hydration layer in the corner, in full analogy with the energy of the hydrocarbon chains.

Within this model, the hydration layer undergoes deformations similar to those of the layer of the hydrocarbon chains, and its energy can be computed analogously to that of the lipid monolayer. At the current stage, we have no information available on the elastic moduli of the hydration layer, but we can draw some general conclusions. First, for deformation of simple bending of a lipid membrane, the layer of the hydrocarbon chains and the hydration layer undergo similar splay. Therefore, the measured bending modulus includes contributions from the chains and from the polar head. According to the experimental results (Leikin et al., 1996; Fuller and Rand, 2001), the values of the bending modulus practically do not depend on the type of polar heads. Hence, the hydration of the heads contributes very little to the membrane splay elasticity. Second, the elastic moduli of a layer scale as powers of its thickness (Helfrich, 1990; Hamm and Kozlov, 2000). The thickness of a hydration layer is about ten times smaller than that of a lipid monolayer (Rand and Parsegian, 1989; Leikin et al., 1993). Hence, the elastic moduli of hydration layer are expected to give a less than 10% contribution to the total moduli of a lipid monolayer.

We are grateful to Leonid Chernomordik for stimulating discussions, critical reading of the manuscript, and constructive suggestions. We thank David Andelman, Samuel Safran, and Michael Schick for helpful discussions. M. K. is grateful to the Israel Science Foundation funded by the Israel Academy of Science and Humanities and the Human Frontier Science Program Organization for the financial support.

REFERENCES

Basanez, G., F. M. Goni, and A. Alonso. 1998. Effect of single chain lipids on phospholipase C-promoted vesicle fusion. A test for the stalk hypothesis of membrane fusion. *Biochemistry.* 37:3901–3908.

Ben-Shaul, A. 1995. Molecular theory of chain packing, elasticity and lipid–protein interaction in lipid bilayers. *In* Structure and Dynamics of Membranes. R. Lipowsky and E. Sackmann, editors. Elsevier Science B. V. 359–401.

Bullough, P. A., F. M. Hughson, J. J. Skehel, and D. C. Wiley. 1994. Structure of influenza hemagglutinin at the pH of membrane fusion. *Nature.* 371:37–43.

Chanturiya, A., L. V. Chernomordik, and J. Zimmerberg. 1997. Flickering fusion pores comparable with initial exocytotic pores occur in protein-free phospholipid bilayers. *Proc. Natl. Acad. Sci. U.S.A.* 94: 14423–14428.

Chen, Z., and R. P. Rand. 1997. The influence of cholesterol on phospholipid membrane curvature and bending elasticity. *Biophys. J.* 73: 267–276.

Chernomordik, L. V., and I. G. Abidor. 1980. The voltage induced local defects in unmodified BLM. *Bioelectrochem. Bioenerg.* 7:617–623.

Chernomordik, L. V., A. N. Chanturiya, J. Green, and J. Zimmerberg. 1994. Monolayer and complete fusion stages of the liposome–planar lipid bilayer interaction dissected by modulation of membrane lipid composition. *Biophys. J.* 66:A144.

Chernomordik, L., A. Chanturiya, J. Green, and J. Zimmerberg. 1995b. The hemifusion intermediate and its conversion to complete fusion: regulation by membrane composition. *Biophys. J.* 69:922–929.

Chernomordik, L. V., V. A. Frolov, E. Leikina, P. Bronk, and J. Zimmerberg. 1998. The pathway of membrane fusion catalyzed by influenza hemagglutinin: restriction of lipids, hemifusion, and lipidic fusion pore formation. *J. Cell Biol.* 140:1369–1382.

Chernomordik, L. V., M. M. Kozlov, G. B. Melikyan, I. G. Abidor, V. S. Markin, and Y. A. Chizmadzhev. 1985. The shape of lipid molecules and monolayer membrane fusion. *Biochim. Biophys. Acta.* 812:643–655.

Chernomordik, L. V., M. M. Kozlov, and J. Zimmerberg. 1995a. Lipids in biological membrane fusion. *J. Membr. Biol.* 146:1–14.

Chernomordik, L. V., E. Leikina, V. Frolov, P. Bronk, and J. Zimmerberg. 1997. An early stage of membrane fusion mediated by the low pH conformation of influenza hemagglutinin depends upon membrane lipids. *J. Cell Biol.* 136:81–94.

De Kruijff, B., and P. R. Cullis. 1980. Cytochrome *c* specifically induces non-bilayer structures in cardiolipin-containing model membranes. *Biochim. Biophys. Acta.* 702:477–490.

Duesing, P. M., R. H. Templer, and J. M. Seddon. 1997. Quantifying packing frustration energy in inverse lyotropic mesophases. *Langmuir.* 13:351–359.

Frank, F. C. 1958. On the theory of liquid crystals. *Discuss. Faraday. Soc.* 25:19–28.

Fuller, N. L., and R. P. Rand. 2001. The influence of lysolipids on the spontaneous curvature and bending elasticity of phospholipid membranes. *Biophys. J.* 81:243–254.

Gaudin, Y. 2000. Rabies virus-induced membrane fusion pathway. *J. Cell Biol.* 150:601–612.

Gawrisch, K., V. A. Parsegian, D. A. Hajduk, M. W. Tate, S. M. Gruner, N. L. Fuller, and R. P. Rand. 1992. Energetics of hexagonal-lamellar-hexagonal transition sequence in dioleoylphosphatidylethanolamine membranes. *Biochemistry.* 31:2856–2864.

Gibbs, J. W. 1876/78. On the equilibrium of heterogeneous substances. *In* The Collected Works of J. Willard Gibbs. vol. 1, New Haven, Yale University Press, 1948.

Gido, P. S., D. W. Schwark, and E. L. Thomas. 1993. Observation of a non-constant mean curvature interface in an ABC triblock copolymer. *Macromolecules.* 26:2636–2640.

Gingell, D., and L. Ginsberg. 1978. Problems in physical interpretation of membrane interaction and fusion. *In* Membrane Fusion. G. Paste and G. L. Nicolson, editors. Elsevier/North-Holland Biomedical Press, 791–833.

Gruen, D. W. R., and S. Marčelja. 1983. Spatially varying polarization in water. A model for the electric double layer and the hydration force. *J. Chem. Soc. Faraday Trans. 2.* 79:225–242.

Gruner, S. M., M. W. Tate, G. L. Kirk, P. T. C. So, D. C. Turner, D. T. Keane, C. P. S. Tilcock, and P. R. Cullis. 1988. X-ray diffraction study of the polymorphic behavior of N-methylated dioleoylphosphatidylethanolamine. *Biochemistry.* 27:2853–2866.

Gruner, S. M. 1989. Stability of lyotropic phases with curved interfaces. *J. Phys. Chem.* 93:7562–7570.

Hamm, M., and M. M. Kozlov. 1998. Tilt model of inverted amphiphilic mesophases. *Eur. Phys. J. B.* 6:519–528.

Hamm, M., and M. M. Kozlov. 2000. Elastic energy of tilt and bending of fluid membranes. *Eur. Phys. J. E.* 3:323–335.

Helfrich, W. 1973. Elastic properties of lipid bilayers: theory and possible experiments. *Z. Naturforsch. C.* 28:693–703.

Helfrich, W. 1990. Elasticity and thermal undulations of fluid films of amphiphiles. *In* Liquids and Interfaces, Les Houches XLVIII 1988, J. Charvolin, J. F. Joanny and J. Zinn-Justin, editors. Elsevier Science Publishers B. V.,

Israelachvili, J. N., S. Marčelja, and R. G. Horn. 1980. Physical principles of membrane organization. *Q. Rev. Biophys.* 13:121–200.

Jahn, R., and T. C. Südhof. 1999. Membrane fusion and exocytosis. *Ann. Rev. Biochem.* 68:863–911.

Kemble, G. W., T. Danieli, and J. M. White. 1994. Lipid-anchored influenza hemagglutinin promotes hemifusion, not complete fusion. *Cell.* 76:383–391.

Kirk, G. L., S. M. Gruner, and D. L. Stein. 1984. A thermodynamic model of the lamellar to inverse hexagonal phase transition of lipid–water system. *Biochemistry.* 23:1093–1102.

Kozlov, M. M., and L. V. Chernomordik. 1998. A mechanism of protein-mediated fusion: coupling between refolding of the influenza hemagglutinin and lipid rearrangement. *Biophys. J.* 75:1384–1396.

Kozlov, M. M., and W. Helfrich. 1992. Effects of cosurfactants on the stretching and bending elasticities of a surfactant monolayer. *Langmuir.* 8:2792–2797.

Kozlov, M. M., S. L. Leikin, L. V. Chernomordik, V. S. Markin, and Y. A. Chizmadzhev. 1989. Stalk mechanism of membrane fusion. Intermixing of aqueous contents. *Eur. Biophys. J.* 17:121–129.

Kozlov, M. M., S. Leikin, and R. P. Rand. 1994. Bending, hydration and interstitial energies quantitatively account for the hexagonal-lamellar-hexagonal reentrant phase transition in dioleoylphosphatidylethanolamine. *Biophys. J.* 67:1603–1611.

Kozlov, M. M., and V. S. Markin. 1983. Possible mechanism of membrane fusion. *Biofizika.* 28:242–247.

Kozlov, M. M., and M. Winterhalter. 1991a. Elastic moduli for strongly curved monolayers. Position of the neutral surface. *J. Phys. II France.* 1:1077–1084.

Kozlov, M. M., and M. Winterhalter. 1991b. Elastic moduli and neutral surface for strongly curved monolayers. Analysis of experimental results. *J. Phys. II France.* 1:1085–1100.

Kuzmin, P. I., J. Zimmerberg, Y. A. Chizmadzhev, and F. S. Cohen. 2001. A quantitative model for membrane fusion based on low-energy intermediates. *Proc. Natl. Acad. Sci. U.S.A.* 98:7235–7240.

Lee, J., and B. R. Lentz. 1997. Evolution of lipidic structures during model membrane fusion and the relation of this process to cell membrane fusion. *Biochemistry.* 36:6251–6259.

Leikin, S. L., M. M. Kozlov, L. V. Chernomordik, V. S. Markin, and Y. A. Chizmadzhev. 1987. Membrane fusion: overcoming of the hydration barrier and local restructuring. *J. Theor. Biol.* 129:411–425.

Leikin S. L., M. M. Kozlov, N. L. Fuller, and R. P. Rand. 1996. Measured effects of diacylglycerol on structural and elastic properties of phospholipid membranes. *Biophys. J.* 71:2623–2632.

Leikin, S., V. A. Parsegian, D. C. Rau, and R. P. Rand. 1993. Hydration forces. *Ann. Rev. Phys. Chem.* 44:369–395.

Leikina, E., and L. V. Chernomordik. 2000. Reversible merger of membranes at the early stage of influenza hemagglutinin-mediated fusion. *Mol. Biol. Cell.* 11:2359–2371.

MacKintosh, F. C., and T. C. Lubensky. 1991. Oriental order, topology and vesicle shapes. *Phys. Rev. Lett.* 67:1169–1172.

Marčelja, S., and N. Radić. 1976. Repulsion of interfaces due to boundary water. *Chem. Phys. Lett.* 42:129–130.

Markin, V. S., M. M. Kozlov, and V. L. Borovjagin. 1984. On the theory of membrane fusion. The stalk mechanism. *Gen. Physiol. Biophys.* 5:361–377.

Melikyan, G. B., J. M. White, and F. S. Cohen. 1995. GPI-anchored influenza hemagglutinin induces hemifusion to both red blood cell and planar bilayer membranes. *J. Cell Biol.* 131:679–691.

Melikyan, G. B., R. M. Markosyan, H. Hemmati, M. K. Delmedico, D. M. Lambert, and F. S. Cohen. 2000. Evidence that the transition of HIV-1 gp41 into a six-helix bundle, not the bundle configuration, induces membrane fusion. *J. Cell Biol.* 151:413–423.

Niggemann, G., M. Kummrow, and W. Helfrich. 1995. The bending rigidity of phosphatidylcholine bilayers. Dependences on experimental method, sample cell sealing and temperature. *J. Phys. II.* 5:413–425.

Nitsche, J. C. C. 1989. Lectures on minimal surfaces. University Press, Cambridge, U.K.

Pantazatos, D. P., and R. C. MacDonald. 1999. Directly observed membrane fusion between oppositely charged phospholipid bilayers. *J. Membr. Biol.* 170:27–38.

Rand, R. P., and N. Fuller. 1994. Structural dimensions and their changes in a reentrant hexagonal-lamellar transition of phospholipids. *Biophys. J.* 66:2127–2138.

Rand, R. P., N. Fuller, S. M. Gruner, and V. A. Parsegian. 1990. Membrane curvature, lipid segregation, and structural transitions for phospholipids under dual-solvent stress. *Biochemistry.* 29:76–87.

Rand, R. P., and V. A. Parsegian. 1989. Hydration forces between phospholipid bilayers. *Biochim. Biophys. Acta.* 988:351–376.

Rawicz, W., K. C. Olbrich, T. McIntosh, D. Needham, and E. Evans. 2000. Effect of chain length and unsaturation on elasticity of lipid bilayers. *Biophys. J.* 79:328–339.

Seddon, J. M. 1990. Structure of the inverted hexagonal (H_{II}) phase, and non-lamellar phase transitions in lipids. *Biochim. Biophys. Acta.* 1031: 1–69.

Siegel, D. P. 1993. Energetics of intermediates in membrane fusion: comparison of stalk and inverted micellar intermediate structures. *Biophys. J.* 65:2124–2140.

Siegel, D. P. 1999. The modified stalk mechanism of lamellar/inverted phase transitions and its implications for membrane fusion. *Biophys. J.* 76:291–313.

Siegel, D. P., J. L. Burns, M. H. Chestnut, and Y. Talmon. 1989. Intermediates in membrane fusion and bilayer/non-bilayer phase transitions imaged by time-resolved cryo-transmission electron microscopy. *Biophys. J.* 56:161–169.

Siegel, D. P., and R. M. Epand. 1997. The mechanism of lamellar-to-inverted hexagonal phase transitions in phosphatidylethanolamine: implications for membrane fusion mechanisms. *Biophys. J.* 73:3089–3111.

Sjölund, M., L. Rilfors, and G. Lindblom. 1989. Reversed hexagonal phase formation in lecithin–alkane–water system with different acyl chain unsaturation and alkane length. *Biochemistry.* 28:1323–1329.

Skehel, J. J., and D. C. Wiley. 2000. Receptor binding and membrane fusion in virus entry: the influenza hemagglutinin. *Ann. Rev. Biochem.* 69:531–569.

Song, L. Y., Q. F. Ahkong, D. Georgescauld, and J. A. Lucy. 1991. Membrane fusion without cytoplasmic fusion (hemi-fusion) in erythrocytes that are subjected to electrical breakdown. *Biochim. Biophys. Acta.* 1065:54–62.

Szleifer, I., D. Kramer, A. Ben-Shaul, W. M. Gelbart, and S. A. Safran. 1990. Molecular theory of curvature elasticity in surfactant films. *J. Chem. Phys.* 92:6800–6817.

Tanford, C. 1980. The Hydrophobic Effect. Formation of micelles and biological membranes. Wiley, New York.

Tate, M. W., and S. M. Gruner. 1987. Lipid polymorphism of mixtures of dioleoylphosphatidylethanolamine and saturated and monosaturated phosphatidylcholines of various chain lengths. *Biochemistry.* 26: 231–236.

Taylor, H. P., S. J. Armstrong, and N. J. Dimmock. 1987. Quantitative relationships between an influenza virus and neutralizing antibody. *Virology.* 159:288–298.

Thomas, T. 1961. Concepts from Tensor Analysis and Differential Geometry. vol. 1. Academic Press, Inc.,

Turner, D. C., and S. M. Gruner. 1992. X-ray reconstitution of the inverted hexagonal (H_{II}) phase in lipid–water system. *Biochemistry.* 31: 1340–1355.

Walter, A., P. L. Yeagle, and D. P. Siegel. 1994. Diacylglycerol and hexadecane increase divalent cation-induced lipid mixing rates between phosphatidylserine large unilamellar vesicles. *Biophys. J.* 66:366–376.

Weaver, J. C., and R. A. Mintzer. 1981. Decreased bilayer stability due to transmembrane potentials. *Phys. Lett.* 86A:57–59.

Winterhalter, M., and W. Helfrich. 1988. Effect of surface charge on the curvature elasticity of membranes. *J. Phys. Chem. US.* 92:6865–6867.